GEOPHYSICS, VOL. 73, NO. 6 (NOVEMBER-DECEMBER 2008); P. WA71–WA82, 11 FIGS.
10.1190/1.2996303

Techniques, analysis, and noise in a Salt Lake Valley 4D gravity experiment

Paul Gettings[1], David S. Chapman[1], and Rick Allis[1]

ABSTRACT

Repeated high-precision gravity measurements using an automated gravimeter and analysis of time series of 1-Hz samples allowed gravity measurements to be made with an accuracy of 5 μGal or better. Nonlinear instrument drift was removed using a new empirical staircase function built from multiple station loops. The new technique was developed between March 1999 and September 2000 in a pilot study conducted in the southern Salt Lake Valley along an east-west profile of eight stations from the Wasatch Mountains to the Jordan River. Gravity changes at eight profile stations were referenced to a set of five stations in the northern Salt Lake Valley, which showed residual signals of <10 μGal in amplitude, assuming a reference station near the Great Salt Lake to be stable. Referenced changes showed maximum amplitudes of -40 through $+40$ μGal at profile stations, with minima in summer 1999, maxima in winter 1999–2000, and some decrease through summer 2000. Gravity signals were likely a composite of production-induced changes monitored by well-water levels, elevation changes, precipitation-induced vadose-zone changes, and local irrigation effects for which magnitudes were estimated quantitatively.

INTRODUCTION

Repeated high-precision gravity measurements track changes in elevation and mass under stations. When gravity changes caused by vertical motion are removed, gravity changes can provide insight into changes of geologic or engineering interest. Examples are changes in storage of groundwater aquifers (Pool and Eychaner, 1995), natural seasonal mass changes (Goodkind, 1986; Keysers et al., 2001), steam field changes under exploited geothermal resources (Isherwood, 1977; Allis and Hunt, 1986; Sugihara, 1999, 2001), or combined mass and elevation changes on volcanic or tectonic systems (Jachens et al., 1981; Arnet et al., 1997; Battaglia et al., 1999; Jousset et al., 2000; Ballu et al., 2003; de Zeeuw-van Dalfsen et al., 2006). The applicability of gravity-change data is controlled by the precision of the gravity changes, which determines the minimum position and mass changes resolvable.

Previously reported measurement techniques (Isherwood, 1977; Whitcomb et al., 1980; Jachens et al., 1981; Dragert et al., 1981; Allis and Hunt, 1986; Hunt and Kissling, 1994; Andres and Pederson, 1993; Arnet et al., 1997; Battaglia et al., 1999; Sasagawa et al., 2003; de Zeeuw-van Dalfsen et al., 2006; Ferguson et al., 2007) generally involve use of manually recorded gravimeters, typically LaCoste & Romberg model D meters (1 μGal reported precision). Notable exceptions are the techniques of Whitcomb et al. (1980) and de Zeeuw-van Dalfsen et al. (2006), who use model G gravimeters (~10 μGal reported precision) to speed surveying over large areal and elevation extents.

Sasagawa et al. (2003) use a three-sensor gravimeter derived from multiple Scintrex CG-3M meters to conduct highly automated ocean-bottom gravimetry. Ferguson et al. (2007) use automated G meters and CG-3M meters with real-time data acquisition and quality checking to minimize the time spent at a station for acceptable accuracy. Previously reported techniques generally use multiple loops of one or more gravimeters to address instrument drift and tare concerns; Sasagawa et al. (2003) use a single loop of three sensors at once. Multiple occupations and/or gravimeters also allow for statistics (typically averaging or linear least-squares fitting) to be applied to reduce measurement errors.

Anticipating increasing interest in repeat gravity monitoring for water resource and reservoir studies, and to improve existing published procedures for conducting high-precision repeated gravity campaigns, we conducted a pilot study in the southern Salt Lake Valley. We designed the method to take best advantage of the development of self-recording (automated) gravimeters and rapid-static GPS to maintain measurement accuracy, compared with existing published techniques, and with minimal equipment and field time.

Manuscript received by the Editor 28 February 2008; revised manuscript received 3 July 2008; published online 20 November 2008.
[1]University of Utah, Department of Geology and Geophysics, Salt Lake City, Utah, U.S.A. E-mail: gettings@earth.utah.edu; david.chapman@utah.edu, david.chapman@gradschool.utah.edu.
[2]Utah Geological Survey, Salt Lake City, Utah, U.S.A. E-mail: rickallis@utah.gov.

For the study, we used a Scintrex CG-3M automated gravimeter for gravity measurements and Trimble geodetic-grade GPS receiver pairs for positioning. Although new techniques were developed with a CG-3M, they are applicable to data collected with any automated gravimeter, such as an Aliod-equipped LaCoste & Romberg meter or the Scintrex CG-5.

Eight stations in a rough east-west transect, spanning the eastern portion of the Salt Lake Valley from the Wasatch Mountains to the Jordan River, were located to acquire field data for technique development and noise characterization. The stations also could track changes in groundwater aquifers caused by municipal pumping and natural recharge, but this was not the principle design goal. Stations were located on existing concrete pads interspersed between municipal supply and monitoring wells, which were measured by the U.S. Geological Survey, Water Resources Division. Locations were chosen on sidewalks and park-building foundations to provide repeatable measurement locations and guarantee access. Five stations were located in the northern Salt Lake Valley to serve as control ("reference") stations; these stations were located far (>1000 m) from pumped wells. The stations span the valley from the Wasatch Mountains to near the Great Salt Lake, and they are expected to respond only to natural seasonal changes.

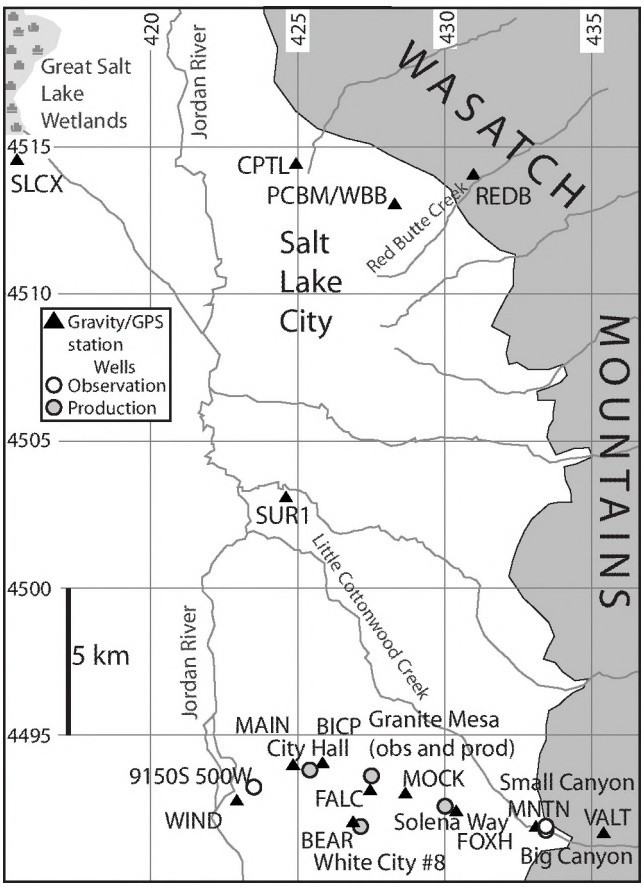

Figure 1. Location of Salt Lake Valley study stations and wells. Gravity and GPS stations are shown as black triangles; wells used in the study are shown as circles (open for monitoring wells, gray for production wells). Gravity stations in the northern valley are used for reference; southern stations compose the east-west profile. Streams are shown where they are above ground. Grid shows UTM coordinates (in km).

The hydrology of the pilot-study area is known to be complicated and spatially heterogeneous (Lambert, 1995). Thus, we designed the pilot study more to provide field data for development of measurement and processing methods than to investigate the detailed hydrogeology of the Salt Lake Valley. Pilot-study results informed us about detection limits for subsequent hydrologic investigations, such as aquifer recharge and storage (see Chapman et al., 2008). The complicated hydrology of the pilot-study area and spatially heterogeneous subsurface, however, provided their own interpretational challenges. Of particular note was the difficulty in choosing a "stable" reference site for computing gravity changes.

SALT LAKE VALLEY PILOT STUDY

The pilot-study area is located in the southern part of Salt Lake Valley, Utah. Gravity stations, monitored wells, GPS stations, and streams are shown in Figure 1. The pilot-study portion of the valley is completely urban, with a dense network of roads and relatively high traffic. However, it also is mainly residential, and this mostly restricts traffic to several main roads, which we avoided when locating stations. Because of development, streams in the valley have been diverted into underground pipes from partway into the valley to the Jordan River.

The pilot-study area has three aquifer systems: a deep confined aquifer underneath the Jordan River, a shallow unconfined aquifer in the top 30 m of fill, and a deep unconfined aquifer between the mountain front and the deep confined aquifer. The deep unconfined aquifer extends from the mountain front toward the center of the valley, where it becomes the deep confined aquifer with the addition of an overlying layer of fine silt and clay. Relatively impermeable layers exist throughout the unconfined aquifer, but in very thin and discontinuous beds that do not significantly disrupt overall permeability. There are local perched aquifers overlying the deep unconfined aquifer, but these are within the upper 30 m of fill.

One particular goal for the pilot study was to determine how many stations could be used in a project, assuming we have no more than two field days to measure gravity at all stations. The two-days-per-campaign constraint requires all stations to be accessible by road, and without laborious entrance requirements.

Gravity data acquisition and analysis

Gravity data for this project were acquired by a Scintrex CG-3M gravimeter, which has a vendor-reported precision of 1 μGal. The control electronics of the CG-3M also apply a suite of corrections to the readings before storage, composed of linear instrument drift, instrument tilt, and temperature compensation.

In this method, each occupation of a station results in a time series of readings. Samples are taken at the instrument-set rate of once per second, for a total of 30 samples. After every 10 samples, the instrument calibrates its internal voltage-sensing circuits, which takes 1 s. The cumulative average and standard deviation of the 30 samples are computed by the instrument and then corrected for instrument tilt according to the electronic tilt sensors and stored constants, linear instrument drift using an empirically updated constant, and temperature variation in the sensor oven. After a 2-s pause, the instrument begins another 30-s cycle. A 30-s cycle, including computations and pause, takes 38 s to complete; typical station occupations take 15 minutes of data, composing ~25 readings.

The 30-s cycle was chosen by inspecting the instantaneous cumulative average of five 60-s cycles; one such cycle is plotted in Figure

2. The cumulative average is recomputed with every sample, along with the standard deviation. No corrections are applied to these statistics during the cycle, but they are applied to the final average. In all five inspected 60-s cycles, the instantaneous average reaches a value within 1 μGal of the final value after the first 30 s. It is more valuable to have more readings of shorter time so as to improve statistical certainty and quality control in processing.

The 15-minute occupation time was chosen to allow short-term instrument transport effects to dissipate while maximizing the number of stations observable in a single field day. A 15-minute time series also gives sufficient data to average out small random noise, such as intermittent vehicle traffic. An example reading time series is shown in Figure 3. For typical field handling of the instrument, transient effects decay within 3 minutes, shown on the figure with a vertical line. Note the large standard deviation envelope in the early readings at a station, resulting from transport effects. During the occupation, there often are intermittent noises associated with traffic or pedestrians, which are seen as individual readings with increased standard deviations; an example is seen on the figure at ~5 min. However, after three minutes from start, the gravity readings are very stable near the average.

The repeatability of gravity measurements is tied directly to the accuracy of meter leveling. All modern gravimeters include electronic levels that aid in accurate leveling. However, because of zero point drift in our CG-3M levels, the tilt meters are reset every two to three months using the procedure detailed in the gravimeter manual. Typical zero point adjustments were 5 arcsec, but they have been as large as 10–20 arcsec. In some cases, the tilt-meter zero points were not updated before a campaign; and the tilt-meter zero points were updated subsequently by more than 10 arcsec. Although it is theoretically possible to correct the tilt correction, accurate values for the zero point errors were not available for old campaigns; so tilt-sensor zero errors were handled by linear detrending during station time-series quality assurance.

As a result of slow changes in the fiber spring and temperature measurement circuit, measured gravity at a stable site drifts over time. This drift is relatively slow and predominantly linear; instrument drift over an 18-day period starting on March 24, 2004, with no meter movement is shown in Figure 4a. Although almost perfectly linear over weeks, the linear rate changes on a timescale of months and therefore is updated at least every three months. Our meter has a complex drift rate history, which is plotted in Figure 4b. The overall decay in drift rate between November 1998 (when the meter was purchased) and April 2004 is expected, because old meters have lower drift rates than new meters (R. Johnston, personal communication, 2001). The excursions to higher drift rates, although apparently seasonal, are unexplained; this behavior has been seen with other CG-3M meters, but without known cause (G. S. Sasagawa, personal communication, 2004).

The CG-3M electronics apply a linear drift correction to each stored reading, based on the difference between the current time and a stored drift start time, and a stored drift coefficient. Errors in the stored drift coefficient result in measurable residual linear drift, which is corrected using the nonlinear instrument drift correction applied during data processing. When the gravimeter is not in use, it is left on a fixed, stable site recording measurements over long intervals (9- or 20-minute cycles). These data are used to update the meter's stored linear drift coefficient by a linear fit to residual drift. The time reset introduces a step change in apparent gravity value at the stable site, and it is the major cause of the need for a known reference (with respect to gravity value) site between gravity campaigns.

Each time series of gravity readings is processed automatically using custom-built software. Raw readings have the Tamura (1987) solid earth tide correction applied; the Longman (1959) correction computed by the instrument, if present, is removed first. We use the Tamura formulation, because it is slightly more accurate than the Longman formula in the meter's electronics (Wenzel, 1996), and applying the correction in processing allows us to use precise geographic coordinates for each station. After the harmonic earth tide correction is applied, there are residual periodic signals evident in long-term records of the meter on a fixed location, possibly resulting from loading effects of the Great Salt Lake. Regardless of cause, the residuals have peak-to-trough amplitudes of ~5 μGal and periods of at least 12 hours. Thus, these residuals are removed by the nonlinear drift function computed as part of the analysis.

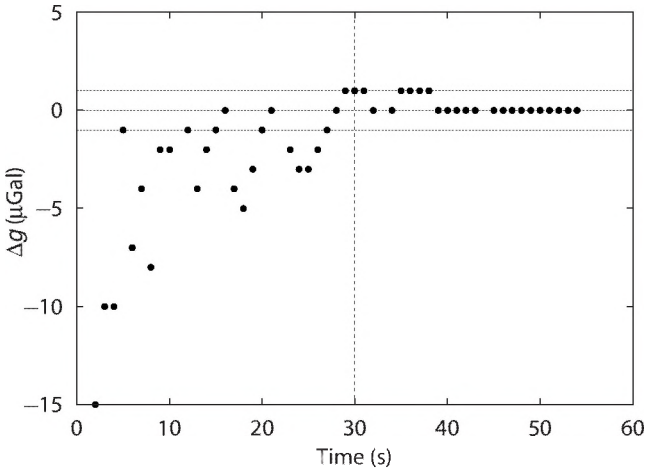

Figure 2. Cumulative average of 1-s gravity samples that produce one reading at a gravity station, differenced from the final average. Clusters of 10 samples are separated by a 1-s calibration pause. Note the small change in the average after 30 s (vertical dotted line), beyond which variation is reduced to ~1 μGal.

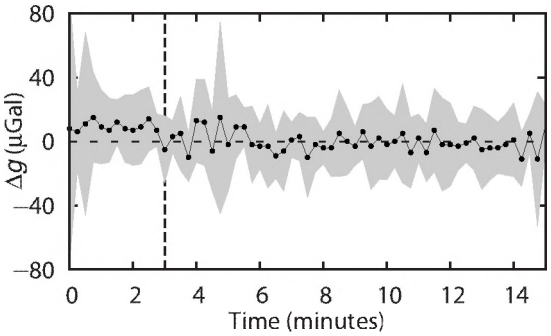

Figure 3. Time series of readings used to compute a gravity value at a single station occupation. Individual readings are shown as dots, differenced from the weighted average of all readings after three minutes. The gray envelope indicates one standard deviation computed from the 30 samples of each reading. The vertical line indicates three minutes from the start.

Station time-series analysis

As an automated check of station occupations, the processing package computes a linear fit to each station occupation time series of readings. If the slope of the linear fit is larger than a defined threshold, chosen empirically to be 97.2 μGal/hr (based on inspection of field stations with noticeable trends), the time series is detrended with the fit slope. The procedure excludes the first three minutes of data and performs a weighted fit using the inverse of reading standard deviations. This detrending effectively pivots the time series about the three-minute reading to have no overall trend in the final 12 minutes of data. Linear trends in the station occupation time series always have resulted from incorrectly set tilt-meter zero positions, with time-varying tilt of the meter. Because earlier readings have smaller tilt, the linear fit removes the effect of changing tilt while maintaining other signals in the time series.

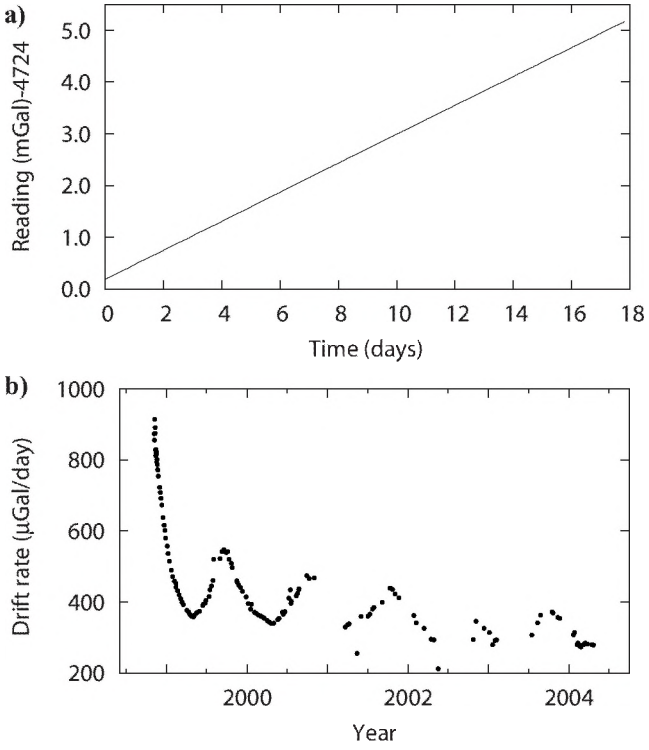

Figure 4. Linear drift characteristics of our CG-3M gravimeter. (a) Drift at a fixed, stable site over 18 days starting 24 March 2004. The linear drift rate is 280 μGal/day. (b) Drift rate between November 1998 and April 2004.

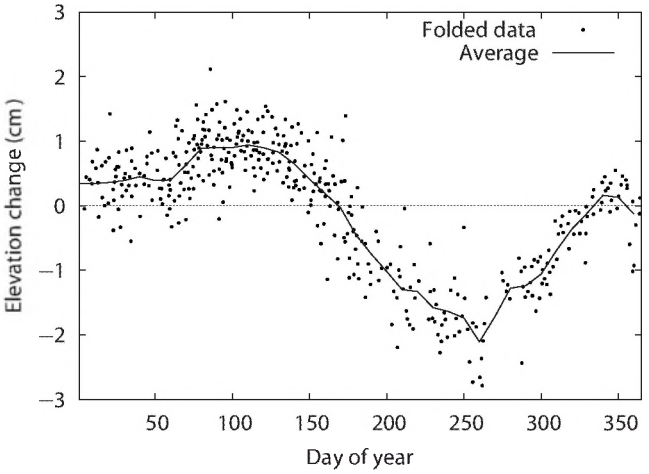

Figure 5. Elevation changes from Meertens et al. (1998) "folded" into a single year and averaged. Points are each elevation residual (in cm) for a given day of the year (day one is 1 January). The line is computed by a running 20-day average.

After linear detrending, the time series is converted to a single weighted average gravity value, where the weights are the inverse square of standard deviations (s.d.) of the readings. Error in the final gravity value from the time series is estimated by twice the standard error of the mean, computed from propagated standard deviations of the readings.

Attempts to improve time-series analysis beyond the weighted average included testing with exponential function fitting and rational function extrapolation algorithms. It was hoped that by using one of these alternate algorithms, it would be possible to obtain a long-duration (15-minute) result from a short (eight-minute) station occupation. Both schemes failed to produce results consistent with weighted averages in at least some real field data; exponential function fits occasionally failed to converge, and other fitting results were more than 5 μGal different from a weighted average. Rational function extrapolation resulted in 5%–10% of field stations with results >5 μGal different from a weighted average. Hence, only weighted averages have been used in the development of the method with pilot-study data.

Elevation-change corrections

After averaging the time series, station occupations are corrected for known elevation changes. The correction is computed from a constant vertical gradient of −3.086 μGal/cm, which is supplied to the processing algorithm. Local vertical gradients can vary from the global free-air gradient (e.g., Arnet et al., 1997), but a variation of 1 μGal/cm, with subsidence known to a few centimeters, causes an error that is still within the acceptable bound of 5 μGal. In addition, measurements of the gradient using multiple heights at a fixed point (our only available gradiometry method) suffer from the limited range of available heights (Butler, 1984) and from extremely local terrain effects, which do not accurately reflect the regional gradient.

For reasons of cost and speed, we used postprocessed rapid-static GPS measurements for elevation control. However, because of restrictions in equipment availability in 1999 and 2000, we could conduct only four GPS campaigns during the project (May and November of 1999 and 2000). These measurements showed no significant elevation change, but they happen to be in periods of the seasonal signal reported by Meertens et al. (1998) with identical elevation. In the absence of subsidence data for most pilot-study campaigns, the data of Meertens et al. (1998) can be used to estimate an elevation correction at the southern Salt Lake Valley stations.

Meertens et al. (1998) established a permanent GPS station at SUR1 (location plotted in Figure 1) between 1996 and 1997; the station was pulled because of seasonal signals just prior to the start of this pilot study. The elevation residual time series from Meertens et al. (1998) is compressed into a single year of data in Figure 5; each year is stacked day by day to form a data set with multiple measurements on each day of the year. Elevation changes are smoothed by a

running 20-day average applied to the folded data. Averaged changes are converted to a gravity change using the global free-air gradient.

Staircase drift function

Instrument drift corrections are inherently empirical calculations, although historically they have been handled by fitting simple theoretical functions to gravity differences. Unfortunately, no particular continuous function is necessarily the best choice for modeling gravimeter drift, which makes the choice of function part of the craft of gravity measurements. For exploration gravity, with acceptable accuracy of 100 μGal, linear drift models often are used for each campaign day.

Previously reported high-precision techniques use large numbers of reoccupations and/or multiple gravity meters to help detect nonlinear instrument drift and tares (e.g., Whitcomb et al., 1980; Jachens et al., 1981; Dragert et al., 1981; Allis and Hunt, 1986; Hunt and Kissling, 1994; Andres and Pederson, 1993; Budetta and Carbone, 1997; Battaglia et al., 1999; Sasagawa et al., 2003; Ferguson et al., 2007), which were removed by fitting of low-order polynomial functions (sometimes with least-squares adjustment, e.g., Jachens et al., 1981). The maximum useful complexity in the drift function is set by available drift information in the campaign, in the form of station reoccupations.

The fundamental assumption of all campaign drift functions is that the value of gravity should not change at a single station over the length of a single campaign. Under this assumption, repeated occupations of stations in a single campaign allow measurement and correction for instrument drift, regardless of cause. The station repeat scheme used in the pilot study is A − B − C − D − E − F − A − B − C − D − E − F − A; note the triple occupation of station *A* during the survey. A better scheme, devised after the end of pilot-study data acquisition, is to use five occupations of the "local base," here called station A: A − B − C − A − D − E − F − A − B − C − A − D − E − F − A. The extra repeats of a local base station allow better representation of highly nonlinear drift curves with any drift function, but particularly with the "staircase" function developed in this paper. The early repeat of station A also allows easier identification of possible tares in the early part of the campaign, compared with the original repeat scheme.

It is important to note that the first station in a survey has zero drift by assumption; there is no information in the survey data to indicate possible errors in the first station. For this reason, a very quiet station always was used as the first occupation of a survey, such as a location where the gravity meter was undisturbed for many hours.

For this pilot study, we developed a novel type of drift function based on arbitrary offsets between stations; a chain of offsets forms a "staircase" function. By construction, the staircase function is nonlinear and discontinuous, handles arbitrary length surveys, and does not assume an a priori functional form of the drift curve. Figure 6 shows a schematic staircase function. The offsets between readings can be viewed as stair steps or linear trends; the drift function is computed only at station occupations, so the behavior of the function between station occupations is irrelevant. The stair-step formulation simplifies the equations (developed in Appendix A), but both views are equally correct. The staircase function produces zero residuals for all surveys in the pilot study (and is therefore error preserving) and automatically adjusts for surveys of arbitrary size.

In addition to the staircase function, best-fit polynomials of as large as degree 6 also were computed for comparison. Polynomial functions worked well for only some campaigns, but they are always subject to nonzero residuals, which increases the error estimate of a station occupation. Campaign days with poor polynomial fits resulted in residuals as large as 20 μGal. With an increasing number of stations (and repeats) in a campaign day, polynomial drift functions must increase in degree to maintain a given level of residual, which leads to concerns over the correct degree for a campaign day.

Because the staircase function faithfully removes drifts between station occupations of arbitrary size, the drift function must be inspected for large offsets that indicate a tare or instrument malfunction. Such offsets are investigated by hand using the field notes, raw reading time series, and surrounding repeat occupations to determine if the offset is an error and which station occupation(s) to discard. Note that by construction, an error at a single occupation cannot contaminate more than that station and its repeats, rather than influencing the drift correction applied to all stations.

Choice of a stable reference station

Instrument drift between surveys is accommodated by assuming one or more stations *stable*, meaning no gravity change over time. Apparent gravity changes at the reference station(s), resulting from instrument drift, provide a correction to the measured gravity changes to compute actual change. Thus, gravity changes at the reference stations are superimposed (in an inverted manner) on all other stations. This superposition can be used to advantage in projects of small spatial extent, so that far-field stations can be used to compute a natural background, enhancing a signal of interest such as infiltration or extraction.

In a study such as this pilot study, which spans tens of kilometers across the hydrologic system, a far-field network would require more stations (10–20 at 15–30-km distances) than we could occupy given the resource constraints. Instead, we chose a set of reference stations spanning the eastern half of the northern Salt Lake Valley. Figure 1 shows locations of the reference stations (REDB, PCBM, WBB, CPTL, SLCX). By using stations in the northern half, which has different (although similar) precipitation and hydrologic conditions compared with the southern Salt Lake Valley, we reduce the

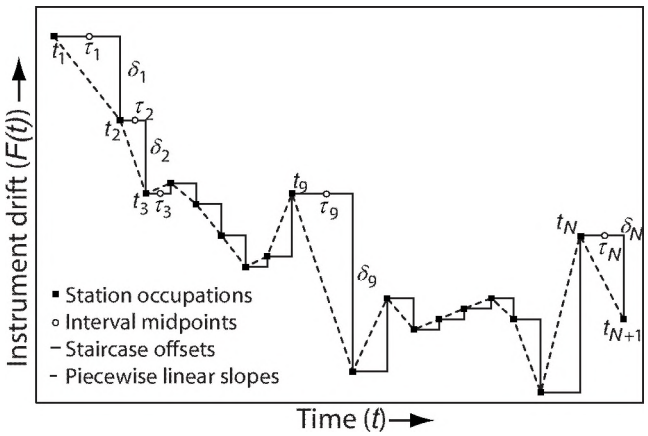

Figure 6. Schematic drift-curve representation by the staircase drift function. Labels refer to the mathematical development in Appendix A; δ_i is the drift for the ith interval, t_i is the time of the ith occupation, and τ_i is the midpoint time of the ith interval.

chance of removing signals of interest caused by identical driving processes. A multistation line from the mountain front to near the Great Salt Lake allows us to use internal consistency measures to reduce the chance of removing signals of interest resulting from a purely local precipitation event or hydrologic influence (e.g., stream leakage, well drawdown).

Based on experience in this pilot study and subsequent projects, it is extremely difficult to find sites that actually are stable at the microgal level in the arid and tectonically active western United States. Sites on bedrock, which normally would be considered stable at the seasonal to interannual scale, can change at seasonal scales because of precipitation; studies using embedded tilt and strain meters inside the granite bedrock of Little Cottonwood Canyon show tilt and strain changes with precipitation (Hantak, 1976) and stream stage of Little Cottonwood Creek (Nye, 1977).

It is difficult to estimate the gravity effect correlated with these tilt and strain changes, but the changes illustrate that bedrock sites might not be as stable as could be expected. Difficulty in estimating the gravity effect comes from uncertainty in the in situ bulk porosity (including fractures) and exact changes in saturation of the bedrock, as no water-level data are available. However, natural groundwater tracer studies have shown that valley recharge is predominantly through bedrock in the southeastern Salt Lake Valley (Manning, 2002), implying that there are likely significant changes in bedrock saturation at seasonal to interannual scales in this pilot-study region, and perhaps in many similar settings in the western United States.

Stations in valley fill are possibly more challenging than those on bedrock, as seasonal and interannual elevation changes on the order of 2–5 cm (6–15 μGal) are added to seasonal and interannual groundwater storage changes. Hence, in this pilot study, we chose the station nearest the Great Salt Lake that is far from wells (pumped or not). We could not find usable bedrock exposures with sufficient access to fit within survey constraints.

In general, reference stations should be determined by the location of absolute gravity measurements during campaigns; gravity changes at reference sites then are measured directly, and the sites do not need to be stable between campaigns. Without access to contemporaneous absolute gravity measurements, any choice of reference station is a balancing act between removing no signals (including instrument drift) and all signals (including those of interest).

GRAVITY RESULTS

Between March 1999 and August 2000, 16 campaigns along the Salt Lake Valley transect were conducted. These gravity campaigns were carried out at approximately four-week intervals, with each field campaign consisting of a single day of measurements. Additional campaigns of a series of reference stations in the north end of the Salt Lake Valley also were conducted during this time, although more sporadically (11 campaigns total).

In May 2000, permission was obtained from the Church of Jesus Christ of Latter-Day Saints to use the Granite Mountain Vaults parking lot as a gravity station (VALT). This station is located on bedrock several kilometers east of the mouth of Little Cottonwood Canyon. With the addition of the Granite Mountain Vaults station, the station at Bicentennial Park (BICP) was dropped from the surveys. Station BICP is very close to Main Park (MAIN), so the loss does not leave any gaps in the survey line.

Of the reference stations in the northern Salt Lake Valley, all were occupied intermittently between March 1999 and August 2000. Two stations are colocated with absolute gravimeter stations measured by the National Geodetic Survey (PCBM and WBB); absolute gravity measurements were performed more than one year before the start of the study, and they have not been used. An additional absolute gravimeter station (SLCJ) also was occupied initially, but the station is too noisy to be of use; it is in front of a store at the Salt Lake City airport, and pedestrian traffic increases the standard deviations of readings to hundreds of microgals. Station SLCJ was not plotted on Figure 1, because no data from the site were used.

Error estimates of the results are computed from error propagation through the reduction algorithm. The total error is dominated by the error in the station time series, typically 2–3 μGal; particularly good occupations have errors of 1–2 μGal. The earth tide correction is accurate through 0.1 μGal, and the staircase drift function does not introduce additional error. Error terms on other possible sources, such as instrument tilt sensitivity, also are below 1 μGal. The error terms are uncorrelated, so the combined error is 5 μGal or less, depending on the time series.

For all campaigns, station SLCX is assumed to be stable, although without either repeated absolute gravity measurements or a set of known stable stations, only internal measures are available for checking actual signal levels at SLCX. Station SLCX was chosen as the stable reference, because it is relatively near (~10.5 km) the Great Salt Lake, not near the Jordan River, which is the primary discharge path, across the Jordan River from other stations and distant from wells. Water-table change at SLCX during the year is probably very small.

Water-level data from February 1999, 2000, and 2001 at the nearest monitored wells (5.25 and 6.18 km distant to the west and east) show water-level declines of 17 cm (~2 μGal at 25% porosity) between 1999 and 2000, and water-level increases of 109 (east) and 187 cm (west) between 2000 and 2001 (U. S. Geological Survey, 2008). Assuming all increase in groundwater level occurs during the spring of 2000 after the well was measured (March through May), the gravity signal from ~1.5 m of water level rise in 25% porosity would be 15–16 μGal. This bounds a likely signal at SLCX, but the signal is not expected to be coherent across the valley to the mountain front because of the spatial heterogeneity of aquifer systems.

From previous studies of the hydrology of the Salt Lake Valley (see Lambert, 1995, for a review), it is clear that the majority of groundwater recharge to valley aquifers occurs at the mountain front. Bedrock flow into the fill accounts for 30%–50%, and stream leakage adds 33% (Manning, 2002). Thus, we expect that stations near Red Butte Creek (REDB) most likely would have the largest gravity-change signals. Stations at the University of Utah (PCBM, WBB) most likely would show a slightly reduced signal compared with REDB, an even smaller signal at CPTL, and the minimum (likely near zero) signal at SLCX. These signals could be coherent, but they do not need to be because of the spatial heterogeneity of the hydrology.

In addition, the Jordan River is the groundwater discharge path for the Salt Lake Valley, making it a groundwater flow barrier. Hence, SLCX (on the west side of the river) responds to changes in the Oquirrh Mountains at the west edge of the Salt Lake Valley, and not to changes in the Wasatch Mountain signals, as the other reference stations do. We expect seasonal gravity-change signals to show decreasing amplitude as distance from the mountain front increases, and SLCX might not be coherent with the other stations. The easiest test is to hold SLCX (which we expect to have near zero signal) constant and inspect changes at the other reference stations.

Figure 7 shows apparent gravity changes at the Salt Lake Valley stations (northern and southern) during the study. Figure 7a (northern stations) illustrates that nearby stations have similar signals (e.g., REDB and PCBM, or PCBM and WBB), but stations with greater separation show less coherence (e.g., PCBM and CPTL). A spatial decay of the signals generally is seen — REDB has the largest signal, with smaller amplitudes at stations PCBM, WBB, and CPTL.

Excluding station REDB, signals along the reference line are bounded to $[-15, 12]$ μGal. So, signals at stations other than SLCX cannot differ from SLCX by more than -15 to as large as $+12$ μGal. These signals could be changing as a result of some coherent driver present across the entire valley; but this is unlikely in the groundwater, because the reference line spans from near (but probably outside) the far side of the primary discharge zone to the mountain-front recharge zone. Precipitation is similar across the northern valley, but it is not sufficient to cause signals in excess of 10 μGal. Thus, it is most likely that the signal at SLCX is small (± 10 μGal) and that the other reference stations are showing seasonal (natural and human-induced) signals.

Figure 7b shows gravity changes at the southern Salt Lake Valley stations, assuming station SLCX is stable. Corrections to the southern stations for instrument drift between campaigns are linearly interpolated from bracketing measurements at SLCX. Gravity changes are in the range of $[-40, 40]$ μGal, with an apparent seasonal drop in summer of 1999 and recovery in winter 1999–2000, but with little change in summer 2000. Because the patterns of individual stations vary significantly, there is not likely to be a single dominant signal swamping local variation. This provides additional support for reference station SLCX being stable and the 40-μGal signals at southern stations being caused by local changes.

It was assumed originally that station VALT, which is located on granite bedrock of the Wasatch Mountains, should provide a stable reference mark for the Salt Lake Valley stations. However, note that in Figure 7b the results for VALT show a 25-μGal signal, assuming station SLCX is stable. If VALT were stable and SLCX variable, changing gravity values at SLCX would be manifested as an apparent signal in VALT. However, the lack of a signal in reference stations over the same time argues that a 20–30-μGal signal at SLCX would have to be very coherent over all stations in the northern valley, which is unlikely (as discussed above).

If VALT were assumed stable, all reference and survey stations would show a sharp decline in the final campaigns. Given that groundwater levels at the nearest wells to SLCX show a rise over the years 2000–2001, a large gravity decline at station SLCX is less likely, even though the survey stations then would agree more closely with expected signals in summer 2000. Given multiple choices of reference, we believe the coherent, albeit scattered, results of the reference stations, added to existing knowledge of the hydrology, argue for station SLCX to be used as the stable reference for all surveys.

Gravity signals at the southern stations are mostly coherent, as they are with the reference stations. This is expected, because stations are installed over one exploited aquifer system. There is a clear seasonal signal of -10 to as large as -40 μGal between March and November 1999, with a significant gravity drop beginning in late April or early May and a recovery in September through November. There is a lesser gravity minimum in late September. The November 1999 peak is followed by a gradual decline from January through April 2000, with a sharp drop in late May 2000 but an equally sharp recovery in June. Stations then decline through August 2000.

GRAVITY EFFECTS QUANTIFIED

Before quantitatively comparing gravity-change results in the southern Salt Lake Valley and water-depth changes in monitoring and production wells, we first correct as necessary for other possible gravity signals at the southern stations. These signals include (1) random error in the measurements; (2) elevation changes resulting from pore-pressure decline and clay drying, or the reverse; (3) systematic errors in the campaigns; and (4) local groundwater or precipitation changes (hydrologic signals) not seen in monitored wells. With the exception of local hydrologic signals, the pilot-study data can bound possible effects of these additional signals. Local hydrologic gravity signals are estimated from water-usage data tracked by the cities. Figure 8 gives a summary of the best-estimate corrected gravity changes, water-level changes, and suite of applied corrections.

Random measurement error

Random error in measurements would have to be present as consistent signals in the station time series; random noise in raw measurements is removed by averaging. Consistent random error in a time series could alter the average, which would result in noticeable, random drifts between repeated occupations. These are not seen in the quality-checked pilot-study data.

Elevation changes

Elevation changes of the reference and southern stations also could introduce unexplained gravity changes. Elevation changes at the reference stations should vary significantly from the mountain-front station (REDB) across the network to the valley-center station (SLCX), based on geodetic GPS studies of the Wasatch Mountains (Chang, 2004) and the results of Meertens et al. (1998). The reference stations also are near the northern edge of the Salt Lake Valley, and thus have thinner (~300-m or less) alluvial deposits compared with the southern stations and the station SUR1 used in Meertens et al. (1998). This elevation-change trend should appear in the gravity changes as a spatial trend along the reference line, which is not seen

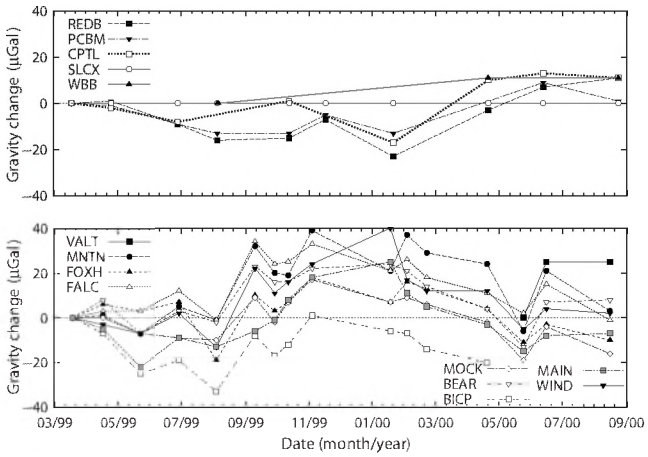

Figure 7. Gravity changes from March 1999 through August 2000 for the pilot-study stations. (a) Reference stations in the northern Salt Lake Valley. Station SLCX is assumed to be stable for all surveys. (b) Gravity changes for southern stations. In both panels, error bars of ~3 μGal are omitted for clarity.

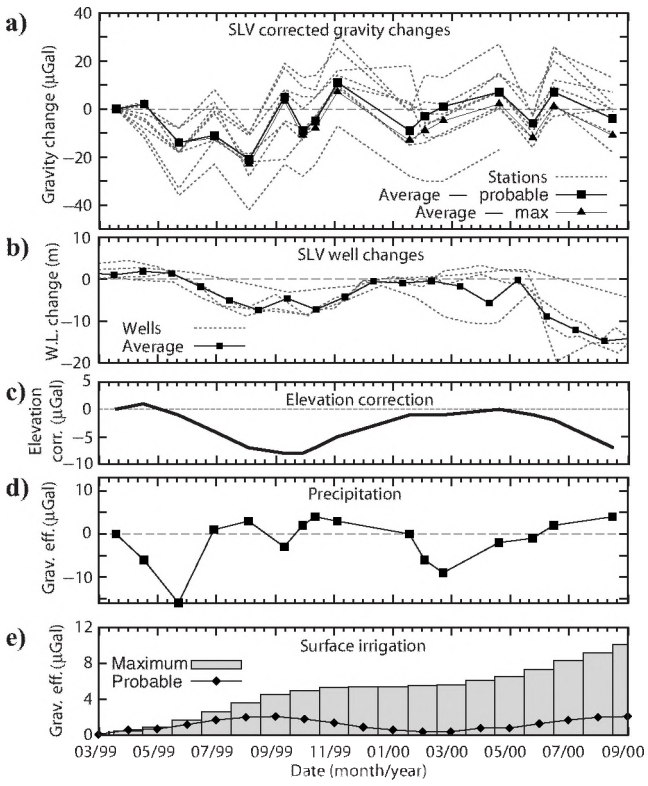

Figure 8. Corrected southern Salt Lake Valley gravity changes, water-level changes, and gravity corrections. Water-level changes are shown for comparison; they are not a correction. Individual corrections are detailed in the text, with only the computed gravity plotted here. The terms *Maximum* and *Probable* for local irrigation effects refer to a maximum possible gravity signal, assuming no groundwater mound decay from irrigation, or the probable gravity effect of irrigation, including a temporal decay term.

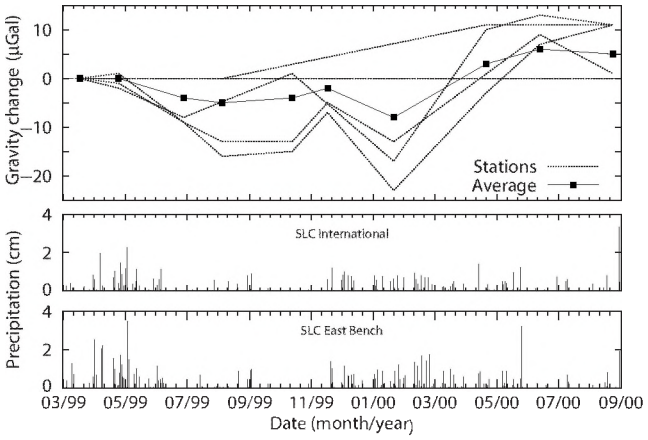

Figure 9. Gravity changes of reference stations and precipitation records for the nearest weather stations. Individual station changes are shown in light dotted lines; the average of all reference stations is shown in the heavy line with points. Error bars, typically 3 μGal, are omitted for clarity. Total daily precipitation data are from the Salt Lake City International Airport and the Salt Lake City East Benches weather stations. Note the seasonality of precipitation, with little rainfall between June and December.

in Figure 7a. Hence, probable elevation change at the reference stations is <3 cm, because reference stations are mostly within 10 μGal of SLCX for all campaigns.

Estimated elevation corrections for the southern gravity stations are computed from the data of Meertens et al. (1998). Elevation corrections, shown in Figure 8c, are subtracted from the southern-station gravity time series; but they are small compared with the signals. Elevation correction increases the gravity decrease during summer 1999 and reduces the gravity increase during fall 1999 and summer 2000.

Systematic errors in campaigns

Systematic errors in the campaigns represent signals present at the reference station assumed to be stable (SLCX). Comparison of the four "floating" reference stations to the assumed stable station should show incoherent "random" signals. The reference stations, plotted in Figure 7a, do show random scatter but not much beyond 10 μGal; this bounds systematic error at SLCX to be $\leq$10 μGal. A signal at the stable reference station (SLCX) that is nearly identical at all other reference stations would not appear in the reference-station plot, but it would appear (inverted) in the southern-station plot. Such a signal, although unexpected because of varying locations of the reference stations, likely would be caused by vadose-zone changes; deep production aquifer changes should not be coherent across the reference stations, because reference stations are not located near production wells. Vadose-zone changes, caused by precipitation, could be coherent across the northern-station line.

Vadose-zone-caused gravity changes should track precipitation in the northern Salt Lake Valley. Figure 9 shows the reference-station gravity changes compared with precipitation records for two weather stations at either end of the reference-station line; East Benches station is just south of the eastern edge of the reference-station line, and Salt Lake City International is on the airport grounds, near station SLCX. There is no consistency between the average reference-station signal (assuming SLCX to be stable) or individual stations and the precipitation record.

Local hydrologic signals

Local groundwater changes resulting from precipitation, water-table changes in local perched aquifers, irrigation (watering lawns), and anisotropic groundwater flow caused by nearby pumping could be invoked to explain signals present in the gravity changes. Without detailed hydrologic information, such as water depths from (nonexistent) monitoring wells under gravity stations and detailed histories of irrigation at stations, local groundwater changes can be only estimated. Precipitation can be reasonably estimated by records from nearby weather stations, but water-level data for the southern stations are unavailable. Local irrigation at sites can be estimated from water-usage records of Sandy City, although only in an average sense.

The gravity effect on the southern stations from local precipitation can be reasonably estimated using an infinite slab approximation. Precipitation along the transect is assumed to be equal to measured precipitation at the Cottonwood Weir weather station. We estimate that 10% of precipitation that falls on the southern valley transect infiltrates into the vadose zone. Assuming that only the last 31 days of precipitation directly affects the gravity changes caused by evapotranspiration, an estimated precipitation signal can be computed by

using a 31-day backward-looking accumulator for each gravity campaign.

The total precipitation, scaled by the infiltration fraction, is used as the thickness for an infinite slab computation. Differencing the precipitation-induced slab effect for a campaign against the baseline value (computed for 19 March 1998) gives an estimated gravity effect of recent precipitation; the effect is negative in summer because spring is the end of the wet season in the valley. Figure 8d plots the southern Salt Lake Valley gravity correction resulting from precipitation. Estimated precipitation gravity effects are relatively small; except for one occasion, they are less than 10 μGal.

Local irrigation at stations, estimated from the total water consumption of Sandy City, is converted to a gravity effect through an infinite slab approximation. Average irrigation on lawns and parks was estimated by averaging monthly water-consumption data for Sandy City between late 2000 and 2004 and concatenating two average years; data from 1999 and early 2000 were not available. Water-consumption data are broken into various categories depending on the water user, and these categories are scaled to account for a portion of consumption indoors. Residential (all types), municipal, school, and commercial water totals are scaled to 67%, reflecting the average indoor consumption of 33% (Millis et al., 2003). Park and landscape water usage are not scaled, as these totals reflect water used entirely for irrigation. Only 10% of the total estimated irrigation water is assumed to reach depths significant for gravity measurements (>30 cm) (K. Solomon, personal communication, 2005).

Scaled monthly irrigation totals, in cubic meters, are converted to an equivalent thickness of a finite (but areally large) slab using an area of 17.4 km^2, which is 30% of the total area of Sandy City. This accounts for the majority of land covered with roads, buildings, and similar facilities. The equivalent slab thickness is used to compute an estimated gravity effect from the Bouguer slab formula, with a density of 1000 $kg \cdot m^{-3}$.

Each month's gravity effect is accumulated to compute a maximum possible gravity effect over the monitoring period. A more probable effect is computed by including exponential decay of the gravity effect (representing subsurface flow outside the measurement zone), with a time constant of two months. Figure 8e shows the maximum (10 μGal) and probable (3 μGal) gravity effects of local irrigation.

Water-level data

The Department of Water Resources at the U.S. Geological Survey in Salt Lake City provided a set of water-depth measurements for this project at wells nearest the gravity stations (Larry Spangler, personal communication, 2001). The well data come from monitoring and production wells, which are between 274 and 1178 m from the nearest gravity station. Depth to water at each well was recorded at varying intervals of approximately four to eight weeks.

Depth change from ground surface to water for all study wells is shown as a function of time in Figure 8b. Wells show clear seasonal signals, ranging from 30 cm through 18 m. Shallow monitoring wells along the survey line show highly variable seasonal signals, ranging from changes of less than 30 cm to as many as 3 m. Production-well data show a more consistent signal of drop between 10 and 18 m during summer. Note that depth change is shown; the depth to water at the start of the plot varies from ~6 m through over 30 m.

Gravity and water-depth correlation

After removing estimated signals at southern stations, the average gravity time series (Figure 8a) is bounded between −30 and 12 μGal; it shows a broad trough in summer 1999 and minor troughs during 2000. The ~15-μGal troughs in June 2000 might represent a response to decreased precipitation or irrigation, or to increased groundwater pumping nearby. There is a delay between the onset of pumping and the gravity drop at stations, which is consistent with a gravity response to pumping at a distance. Regardless of whether the small troughs in late 1999 and 2000 are pumping induced, there is a change in gravity response of the southern Salt Lake Valley stations between summer 1999, when there is a clear average gravity signal tracking pumping, and 2000, when there is no clear average gravity signal.

Evapotransporation (ET) of soil moisture also could affect gravity changes measured in the southern-station transect. However, the mapping between ET and a gravity effect is not intuitively clear, and measurements of the ET rate are not available for the southern-station transect. However, ET should scale with average daily temperature, which allows qualitative evaluation of ET in the gravity signal. Figure 10b plots the average daily temperature at the Cottonwood Weir weather station, at the east end of the transect between stations MNTN and VALT. Comparison with the corrected gravity signal shown in Figure 10a does not indicate a clear tracking; gravity drop in 1999 during summer high temperatures is not seen in 2000, even though temperatures are nearly identical. Hence, ET is not likely a major component of the gravity signal at southern valley stations.

Although groundwater levels at wells to the east and west of SLCX show little change during the pilot study, there is a remote possibility that station SLCX is affected by changes in the Great Salt Lake during the pilot study. Figure 10c shows elevation change of the lake, relative to the level of 18 March 1999. Assuming that changes in lake level are transferred completely to a change in water level under SLCX, an infinite slab computation for a change of

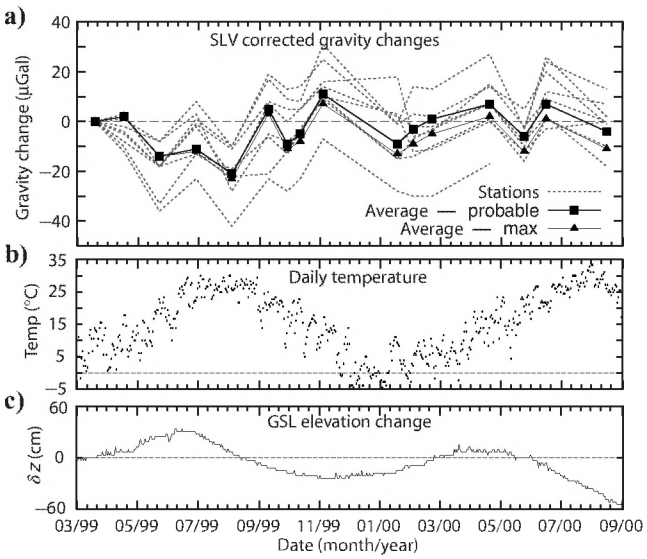

Figure 10. Gravity changes of the southern Salt Lake Valley transect compared with temperature and Great Salt Lake levels. (a) Corrected gravity changes. (b) Daily average temperatures at the mouth of Little Cottonwood Canyon (station MNTN). (c) Great Salt Lake elevation change (in cm) from the level of 18 March 1999.

60 cm yields a gravity effect of 6 μGal. This signal is not significant, even if present, which is unlikely because of the groundwater-level records.

To assess tracking of each gravity station with the nearest well, instead of the average gravity and well signals, we compute a crosscorrelation between each gravity survey and water-depth data interpolated between bounding measurements. We compute the correlation after inverting the sign of depth changes, producing a positive correlation between water-level rise (negative depth) and gravity increases. Figure 11 shows correlation results for offsets of as many as 270 days.

Of all gravity stations with wells within 800 m, only station MNTN shows a high correlation with near well(s). However, correlation peaks at ~120 days are significantly smaller for the nearest well (Small Canyon) and largest for the farther well. The otherwise low or negative correlations for stations with their nearest wells indicate that individual-station gravity changes are not representative of the nearest well-water depth changes. This is not particularly unexpected, given the distances to wells (~300 m through ~800 m) in a region with very complex near-surface hydrogeology. That the best correlation was obtained between a gravity station near the mouth of the canyon (where there are few production wells) and shallow unpumped wells indicates that both signals are responding to the same driving changes, but the gravity station has a time lag of ~4 months.

Without records of shallow- and deep-aquifer water levels directly under the gravity stations, or elevation changes at the stations during campaigns, it is not possible to proportion conclusively the signals (or lack thereof) seen at the southern Salt Lake Valley stations to various causes. It is unlikely that random or systematic errors are significant factors in the apparent signals; but it is probable that the changing nature of the time series results from the combination of local geology controlling fluid flow, subsidence caused by natural and induced groundwater changes, mass change caused by production, local precipitation anomalies, and near-station irrigation.

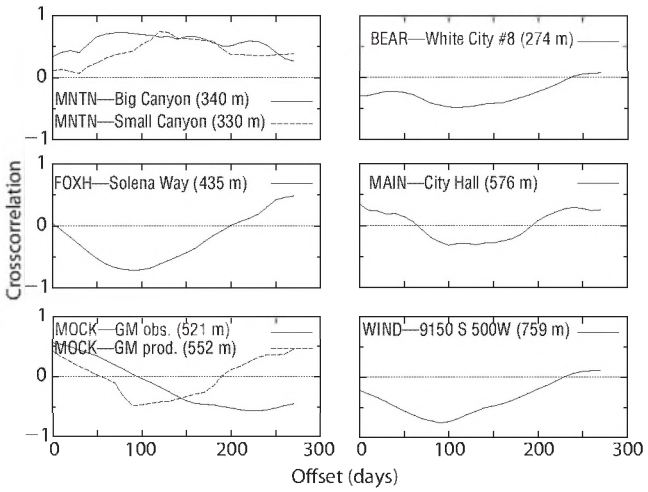

Figure 11. Crosscorrelation results for offsets of as many as 270 days. Each gravity station with a nearby well is correlated to the well, with the distance to the well given in parentheses after the well name. Note that only station MNTN shows high correlation at any offset, although the canyon wells have water-depth changes of <1 m during the pilot study.

CONCLUSIONS

Results from a 4D gravity study in the Salt Lake Valley conducted over an 18-month period permit the following observations and conclusions.

Collecting a time series of gravity measurements at each station occupation allows automated data processing that enhances quality assurance and highly precise gravity estimation. By averaging ~20 readings with standard deviations of 10–40 μGal each, we achieved a station occupation precision (as measured by two standard errors) of 2–3 μGal. In addition, inspection of the time series from an occupation allows the possibility of improving the data series; examples are detrending time series to remove effects of level drift or ignoring the first few minutes of data to remove transportation effects in the gravimeter.

A staircase drift function also aids precision by providing a scalable, error-preserving function to handle all types of instrument drift: linear, nonlinear, and tare. Because the staircase drift function does not require an a priori functional form, it scales without change from surveys with only linear drift information (single base loops) to multiday campaigns with multiple occupations of every station. Combined with a repeat scheme that provides loops throughout a survey day, the staircase function also provides a good approximation to extremely nonlinear drift functions that might result from transportation, instrument noise, or uncorrected periodic signals (e.g., earth tides).

This pilot study yielded gravity changes that were accurate and precise to 5 μGal, but reflecting a complex convolution of signals at multiple time and space scales. Gravity changes at eight profile stations were referenced to a set of five stations in the northern Salt Lake Valley, which show residual signals of <10 μGal in amplitude, assuming a reference station near the Great Salt Lake to be stable. Referenced changes show maximum amplitudes of -40 through $+40$ μGal at profile stations, with minima in summer 1999, maxima in winter 1999–2000, and some decrease through summer 2000.

In the study, we were challenged to find a single, stable gravity base station at the microgal level. Bedrock sites along Basin and Range valley borders might have stability problems because of pervasive faulting and active extension, and from active groundwater systems providing recharge to the valleys. We counteracted the lack of absolute gravity measurements during the campaigns in part through the use of a widely separated set of reference stations.

Results of the Salt Lake Valley pilot study provided quantitative estimates of noise sources, signal amplitudes, and data-processing issues that should guide experiment design for future studies in similar terrain. Phenomena and typical signal-amplitude estimates include field measurement accuracy, including instrument noise, 5 μGal; elevation changes, 10 μGal; precipitation, 5 μGal; surface irrigation, 2 μGal. Projects with an expected signal of <40 μGal will require the acquisition of data to measure these signals.

The groundwater system of the southern Salt Lake Valley does not produce a simple annual gravity effect, as might be expected from groundwater withdrawal in the growing season and springtime recharge from mountain runoff. To deconvolve the local and background signals from groundwater signals of interest, it would be necessary to better understand the particulars of confined versus unconfined aquifers in the project area and to collect detailed information on precipitation, evapotranspiration, and near-station vadose- and saturated-zone hydrologic conditions.

ACKNOWLEDGMENTS

We thank Larry Spangler at the U. S. Geological Survey for collecting the well-level data during the study. Interpretation was aided by discussions with Kip Solomon at the University of Utah. Our gravimeter was provided by the Energy & Geoscience Institute at the University of Utah, and the original GPS equipment was borrowed from UNAVCO. Several anonymous reviewers helped improve the paper.

APPENDIX A

STAIRCASE DRIFT FUNCTION

We construct a staircase drift function as follows. First we label all station occupations with a number i, starting at 1. We define n as the total number of station occupations in the survey ($n = 13$ for the example repeat scheme); thus, there are $N = n - 1$ intervals between occupations. Let g_i be the gravity reading and t_i the time of the ith occupation. For every interval between two sequential occupations, we define τ_k as the midpoint time; note that there are N such times.

The drift function, $F(t)$, is defined as

$$F(t) = \sum_{k=1}^{N} C_k(t)\,\delta_k, \tag{A-1}$$

where $C_k(t)$ is the coefficient for the kth interval taken from the set $\{0,1\}$, and δ_k is the drift for that interval. Note that the length of the interval is not used, nor are there any constraints on the change between sequential δ_k values. Thus, the function $F(t)$ is immediately applicable to surveys of arbitrary size and duration.

The value of $C_k(t)$ is found from

$$C_k(t) = \begin{cases} 0 & t < \tau_k \\ 1 & t \geq \tau_k \end{cases}. \tag{A-2}$$

We label stations and repeat occupations with subscripts, so the first occupation of station A becomes A_0, the first repeat of station A becomes A_1, the second A_2, and so on. Next we construct a mapping, $\Gamma(\alpha_k) = i$, where α_k varies over all stations (α) and occupations of the station ($k = (0,1,\ldots)$), and i represents the occupation number; this mapping is used below to build the drift observation equations. As an example, for the local base of the pilot-study repeat scheme, the mappings are $\Gamma(A_0) = 1$, $\Gamma(A_1) = 9$, and $\Gamma(A_2) = 13$.

A set of δ_k must be found so that the equation set

$$D_{\Gamma(\alpha_k)\Gamma(\alpha_{k+1})} = [g_{\Gamma(\alpha_{k+1})} - F(t_{\Gamma(\alpha_{k+1})})] - [g_{\Gamma(\alpha_k)} - F(t_{\Gamma(\alpha_k)})] \tag{A-3}$$

is minimized for all α_k (stations and repeated occupations).

This inversion problem is generally underdetermined; there are $n - 1$ unknowns, and at most $n/2$ equations. Additional equations result from noting that the difference between stations should be constant over a campaign. Hence, we construct additional difference-of-differences equations:

$$D_{\Gamma(\alpha_k)\Gamma(\alpha_{k+1})\Gamma(\alpha_j)\Gamma(\alpha_{j+1})} = D_{\Gamma(\alpha_{k+1})\Gamma(\alpha_{j+1})} - D_{\Gamma(\alpha_k)\Gamma(\alpha_j)}, \tag{A-4}$$

where k and j can vary over all stations that have repeated occupations. To remove redundant equations, only differences that are forward in time are used; that is, only pairs of stations where the time of occupation $\Gamma(\alpha_j)$ is later than that of occupation $\Gamma(\alpha_k)$.

Note also that if a station has multiple repeated occupations, these are used by forming the above equation once for each repeat with the original occupation. If the survey does not have enough repeated stations, the problem still might be underdetermined, even with the differences of differences. Results of an underdetermined system might still be valid; in all work so far, inversion matrices have been nonsingular, even with an underdetermined problem.

Define M as the total number of equations, or the number of equations for repeated occupations plus the number of equations for interstation differences. To solve the (most likely) overdetermined minimization problem, it is convenient to recast it into a matrix form and add data weighting factors. The vectors $\hat{m}$ and $\hat{d}$ are defined by

$$\hat{m} = [\delta_1, \delta_2, \ldots, \delta_N]^T \tag{A-5}$$

$$\hat{d} = [D_{11'}, D_{22'}, \ldots, D_{121'2'}, \ldots]^T, \tag{A-6}$$

and the $M \times N$ operator matrix $\hat{A}$ is defined by

$$\hat{A} = [A_{lm}], \tag{A-7}$$

where A_{lm} is chosen according to the following algorithm. If l is a row with an equation for a repeated occupation, then

$$A_{lm} = \begin{cases} 1 & t_i < t_m < t_{i'} \\ 0 & \text{otherwise} \end{cases}, \tag{A-8}$$

where i is the occupation and i' the repeated occupation represented by the lth row.

If row l is a difference-of-differences equation, then

$$A_{lm} = \begin{cases} -1 & t_i < t_m < t_j \\ 0 & t_{i'} < t_m < t_j \\ 1 & t_{i'} < t_m < t_{j'} \\ 0 & \text{otherwise} \end{cases}, \tag{A-9}$$

where i, i', j, and j' are the occupations and repeats represented by the lth row. Define the square $M \times M$ data weighting matrix by

$$\hat{W} = [W_{ll}], \tag{A-10}$$

where W_{ll} is computed by the following algorithm: If row l is a repeated occupation equation,

$$W_{ll} = \frac{1}{\sqrt{\sigma_i^2 + \sigma_{i'}^2}} \tag{A-11}$$

otherwise,

$$W_{ll} = \frac{1}{\sqrt{\sigma_i^2 + \sigma_{i'}^2 + \sigma_j^2 + \sigma_{j'}^2}}, \tag{A-12}$$

where i, i', j, and j' are the occupations and repeats represented by the lth row.

The matrix equation to be solved is

$$\hat{W}\hat{A}\hat{m} = \hat{W}\hat{d}. \tag{A-13}$$

As the operator is linear, the problem can be solved in a direct linear least-squares inversion, which can be written in matrix notation as

$$\hat{m} = (\hat{A}^T\hat{W}^2\hat{A})^{-1}\hat{A}^T\hat{W}^2\hat{d} = \hat{Q}^{-1}\hat{A}^2\hat{W}^2\hat{d}, \quad \text{(A-14)}$$

where $\hat{Q}$ is the diagonal matrix found from the singular value decomposition of $\hat{A}$.

When $\hat{m}$ is found by equation A-14, the drift for any station can be computed from a specialization of equation A-1. As the drift function always is being computed on an interval boundary,

$$F(t_k) = F(k) = \sum_{i=1}^{k-1} \delta_i. \quad \text{(A-15)}$$

For stations that have no repeats, the inversion process (being a least-squares process) assigns a drift value that is a linear interpolation between the nearest repeated stations.

REFERENCES

Allis, R., and T. Hunt, 1986, Analysis of exploitation-induced gravity changes at the Wairakei geothermal field: Geophysics, **51**, 1647–1660.

Andres, R. S., and J. R. Pederson, 1993, Monitoring the Bulalo geothermal reservoir, Philippines, using precision gravity data: Geothermics, **22**, 395–402.

Arnet, F., H.-G. Kahle, E. Klingele, R. B. Smith, C. M. Meertens, and D. Dzuirsin, 1997, Temporal gravity and height changes of the Yellowstone caldera, 1977–1994: Geophysical Research Letters, **24**, 2741–2744.

Ballu, V., M. Diament, P. Briole, and J.-C. Ruegg, 2003, 1985–1999 gravity field variations across the Asal Rift: Insights on vertical movements and mass transfer: Earth and Planetary Science Letters, **208**, 41–49.

Battaglia, M., C. Roberts, and P. Segall, 1999, Magma intrusion beneath Long Valley caldera confirmed by temporal changes in gravity: Science, **285**, 2119–2122.

Budetta, G., and D. Carbone, 1997, Potential application of the Scintrex CG-3M gravimeter for monitoring volcanic activity: Results of field trials on Mt. Etna, Sicily: Journal of Volcanology and Geothermal Research, **76**, 199–214.

Butler, D. K., 1984, Interval gravity-gradient determination concepts: Geophysics, **49**, 828–832.

Chang, W.-L., 2004, GPS (global positioning system) studies of the Wasatch fault zone, Utah, with implications for elastic and viscoelastic fault behavior and earthquake hazard: Ph.D. thesis, University of Utah.

Chapman, David. S., Eric Sahm, and Paul Gettings, 2008, Monitoring aquifer storage and recovery using repeat gravity measurements: The Weber River project, Utah: Geophysics, this issue.

de Zeeuw-van Dalfsen, E., H. Rymer, G. Williams-Jones, E. Sturkell, and F. Sigmundsson, 2006, Integration of micro-gravity and geodetic data to constrain shallow system mass changes at Krafla Volcano, N Iceland: Bulletin of Volcanology, **68**, 420–431.

Dragert, H., A. Lambert, and J. Liard, 1981, Repeated precise gravity measurements on Vancouver Island, British Columbia: Journal of Geophysical Research, **86**, 6097–6106.

Ferguson, J. F., T. Chen, J. Brady, C. L. V. Aiken, and J. Seibert, 2007, The 4D microgravity method for waterflood surveillance II — Gravity measurements for the Prudhoe Bay reservoir, Alaska: Geophysics, **72**, no. 2, I33–I43.

Goodkind, J. M., 1986, Continuous measurement of nontidal variations of gravity: Journal of Geophysical Research, **91**, 9125–9134.

Hantak, F. J., 1976, Correlation of strain and tilt episodes with local precipitation: M.S. thesis, University of Utah.

Hunt, T. M., and W. M. Kissling, 1994, Determination of reservoir properties at Wairakei geothermal field using gravity change measurements: Journal of Volcanology and Geothermal Research, **63**, 129–143.

Isherwood, W., 1977, Geothermal reservoir interpretation from change in gravity: Presented at the Third Workshop on Geothermal Reservoir Engineering, Stanford University.

Jachens, R., D. Spydell, G. Pitts, D. Dzurisin, and C. Roberts, 1981, Temporal gravity variations at Mount St. Helens, March-May 1980: U. S. Geological Survey Professional Paper 1250, 175–181.

Jousset, P., S. Dwipa, F. Beauducel, T. Duquesnoy, and M. Diament, 2000, Temporal gravity at Merapi during the 1993–1995 crisis: An insight into the dynamical behavior of volcanoes: Journal of Volcanology and Geothermal Research, **100**, 289–320.

Keysers, C. J., H. J. Kuempel, and J. Campbell, 2001, Local seasonal gravity changes in the Lower Rhine Embayment, Germany: Acta Geodaetica et Geophysica Hungarica, **36**, 313–326.

Lambert, P., 1995, Numerical simulation of ground-water flow in basin-fill material in Salt Lake Valley, Utah: Technical Publication 110-B, Utah Department of Natural Resources.

Longman, I., 1959, Formulas for computing the tidal accelerations due to the moon and sun: Journal of Geophysical Research, **64**, 2351–2355.

Manning, A., 2002, Using noble gas tracers to investigate mountain-block recharge to an intermountain basin: Ph.D. thesis, University of Utah.

Meertens, C., R. Smith, W. Chang, C. Puskas, and T. V. Hove, 1998, GPS-derived deformation of the western U.S. Cordillera, Wasatch Front, Utah, and Yellowstone: Eos, Transactions, American Geophysical Union, **79**, F203.

Millis, E., E. Klotz, T. Stonely, M. Waters, and L. Summers, 2003, Utah's M&I water conservation plan: Investing in the future: Technical report, Utah Division of Water Resources.

Nye, R. K., 1977, Causes of observed variations in strain and tilt at the Granite Mountain records vault, Salt Lake County, Utah: M.S. thesis, University of Utah.

Pool, D., and J. Eychaner, 1995, Measurements of aquifer-storage change and specific yield using gravity surveys: Ground Water, **33**, 425–432.

Sasagawa, G. S., W. Crawford, O. Eiken, S. Nooner, T. Stenvold, and M. A. Zumberge, 2003, A new sea-floor gravimeter: Geophysics, **68**, 544–553.

Sugihara, M., 1999, Continuous gravity measurements for reservoir monitoring: Presented at the Proceedings, 24th Workshop on Geothermal Reservoir Engineering, Stanford University.

———, 2001, Reservoir monitoring by repeat gravity measurements at the Sumikawa geothermal field, Japan: Presented at the Proceedings, 26th Workshop on Geothermal Reservoir Engineering, Stanford University.

Tamura, Y., 1987, A harmonic development of the tide-generating potential: Bulletin d'Informations Marées Terrestres, **99**, 6813–6855.

U.S. Geological Survey, 2008, National Water Information System (NWISWeb), http://waterdata.usgs.gov/nwis, accessed 10 April 2008.

Wenzel, H., 1996, Accuracy assessment for tidal potential catalogs: Bulletin d'Informations Marées Terrestres, **124**, 9394–9416.

Whitcomb, J. H., W. O. Franzen, J. W. Given, J. C. Pechman, and L. J. Ruff, 1980, Time-dependent gravity in southern California, May 1974 to April 1979: Journal of Geophysical Research, **85**, 4363–4373.